Wood Physics/Mechanical Properties

Kazuki Uehara, Hiroaki Horiyama, Yuka Miyoshi*, Kana Yamashita, Keisuke Kojiro and Yuzo Furuta

Mechanism of changes in the mechanical properties of wood due to water adsorption and desorption described by rheological considerations

https://doi.org/10.1515/hf-2024-0114
Received November 28, 2024; accepted April 15, 2025;
published online April 29, 2025

Abstract: This study investigates the rheological mechanisms underlying changes in the mechanical properties of wood during moisture adsorption and desorption. To approximate the net molecular momentum at a specific humidity and time, an index was established by dividing the loss tangent value under equilibrium conditions at each humidity by the loss tangent value at each time point. This approach linked the unstable microstructural behavior associated with adsorption and desorption to the stabilization of the structure over time and molecular mobility at specific conditions. This metric enabled effective tracking of molecular mobility during humidity changes and provided insights into the mechanisms driving changes in mechanical properties. During adsorption, wood transitions from a glassy state far from the rubbery state toward one closer to the rubbery state, while desorption shows the opposite trend. Results also indicated an energy barrier near the medium humidity (30–60 %RH), unrelated to lignin. Instead, the softening of hemicellulose and changes in amorphous polymer states within the cell wall likely play critical roles in these mechanical property changes.

Keywords: dynamic viscoelasticity; adsorption/desorption process; glass transition temperature; hemicellulose; energy barriers

***Corresponding author: Yuka Miyoshi**, Department of Wood Properties and Processing, Forestry and Forest Products Research Institute, Matsunosato 1, Tsukuba, Ibaraki 305-8687, Japan, E-mail: ymiyoshi@ffpri.affrc.go.jp
Kazuki Uehara, **Keisuke Kojiro and Yuzo Furuta**, Division of Environmental Sciences, Graduate School of Life and Environmental Sciences, Kyoto Prefectural University, Shimogamohangi-cho, Sakyo-ku, Kyoto 606-8522, Japan, E-mail: s823732001@kpu.ac.jp (K. Uehara), kojiro@kpu.ac.jp (K. Kojiro), furuta@kpu.ac.jp (Y. Furuta)
Hiroaki Horiyama, National Institute of Advanced Industrial Science and Technology (AIST), Multi-Material Research Institute, Nagoya, Aichi 463-8560, Japan, E-mail: h.horiyama@aist.go.jp
Kana Yamashita, Department of Wood Properties and Processing, Forestry and Forest Products Research Institute, Matsunosato 1, Tsukuba, Ibaraki 305-8687, Japan, E-mail: zaikana@ffpri.affrc.go.jp

1 Introduction

The relationship between the physical properties of wood and water adsorption has long been a subject of research (Skaar 1988). However, advancements in measurement technologies have revealed that the correlations between molecular mobility and sorption isotherms could not be explained by previous theories or experiments, indicating the need for more detailed investigations (Engelund et al. 2013; Thybring et al. 2022). When a material under load experiences fluctuating moisture conditions, it undergoes accelerated creep compared to constant humidity conditions, which is known as mechano-sorptive (MS) creep, and numerous studies have been conducted to investigate this behavior (Armstrong and Christensen 1961; Grossman 1976; Hunt and Gril 1996; Hunt and Shelton 1987; Leicester 1971; Mukudai and Yata 1988; Nakano 1996; Takemura 1968; Tokumoto 2001; Olsson et al. 2007). Furthermore, a unified explanation of MS creep has been proposed based on the concept of wood destabilization, suggesting that the load may not be essential for abnormal deformation during the moisture change process (Takahashi et al. 2004, 2005, 2006).

Wood destabilization occurs (immediately or slowly) after changes in environmental conditions due to the wood failing to reach an equilibrium state (Brémaud and Gril 2021a,b; Hunt and Gril 1996; Iida et al. 2002; Ishimaru et al. 2001a,b,c). It was demonstrated that even when the moisture content of the wood is constant, the amount of creep deformation immediately after a change in humidity is greater than that after the wood has been left at a constant humidity for a long period (Takahashi et al. 2004, 2005). Experimental

results have demonstrated that the wood is unstable immediately after a humidity change, and it takes time to reach a stable state at that humidity. Therefore, fast humidity changes do not provide sufficient time for the wood to stabilize, resulting in significant short-term instability.

Previous studies have reported MS creep in terms of the destabilization of wood in the relaxation process with different adsorption and desorption times; however, they have not directly explained the underlying mechanisms. Specifically, these studies do not investigate the relationship between molecular motion, such as changes in the microstructure associated with adsorption and desorption, the activity of molecules at different moisture contents, and the mechanical relaxation derived from individual wood components. In order to clarify the changes in the mechanical properties of wood associated with the adsorption and desorption of water molecules, this study measured the dynamic viscoelasticity of wood under various humidity change scenarios. This is based on previous studies on the temperature dependence of the rheological properties of wood (Becker and Noack 1968; Furuta et al. 1995, 1997, 2001, 2008, 2010; Horiyama et al. 2022; Kojiro et al. 2008a,b,c; Miyoshi et al. 2018, 2020, 2024; Obataya et al. 1996; Salmén 1984; Salmén et al. 2016).

It is well established that the thermal softening temperature of wood depends on the moisture content (Becker and Noack 1968; Furuta et al. 2001). Becker and Noack (1968) investigated the relationship between temperature, moisture content, and viscoelastic properties (torsional modulus and logarithmic damping ratio) of wood samples through transverse dynamic torsional viscoelasticity tests conducted at thermal/humidity equilibrium conditions. Within the temperature range of 0–100 °C, the fully dry wood samples did not exhibit a temperature-dependent peak in the logarithmic damping ratio. However, when the moisture content exceeded 12 %, a clear peak was observed within the same temperature range. As moisture content increased, the peak in the logarithmic damping ratio shifted to lower temperatures while the peak value decreased. Furthermore, it has been suggested that the thermal softening of saturated wood is linked to the glass transition of lignin (Furuta et al. 2008, 2010; Salmén 1984). Consequently, it can be inferred that at temperatures below the thermal softening point, lower moisture contents result in a greater difference from the glass transition temperature; that is, at higher moisture contents, the wood is closer to the rubbery state rather than the glassy state.

The aim of this paper was to clarify the changes in the mechanical properties of wood during the adsorption and desorption process from the perspective of rheology. To this end, this paper discusses how the change in fluidity over time after adsorption and desorption can be explained consistently from the two perspectives of stabilization and molecular motion. In addition, this paper discusses the mechanism of the change in dynamic viscoelasticity during the adsorption and desorption processes, as the viscous behavior changes around 60 % RH.

2 Materials and methods

2.1 Specimen preparation

The wood species used was hinoki (*Chamaecyparis obtusa*), specifically the heartwood just inside the sapwood. The wood was sourced from sections that were straight in the longitudinal direction and free of cross-grains. Figure 1(a) shows an illustration of the test specimens. The specimens measured 26 mm in the radial direction (*R*), 3 mm in the tangential direction (*T*), and 1 mm in the longitudinal direction (*L*). A total of 28 specimens were consecutively cut in the *L* direction. The specimens were alternately allocated for dynamic viscoelasticity measurements and moisture content measurements, 14 specimens each. The average annual ring width of the specimens was 0.73 mm, and their oven-dry density was 410 kg/m^3.

The specimens were extracted using methanol in a Soxhlet extractor for 9 h to remove wood extractives components, and then air-dried in a fume hood for 3 days. After extraction and drying, the specimens were saturated with distilled water at 20 °C for 60 min under alternating decompression at 0.1 MPa. To ensure uniform drying history, the specimens were boiled in distilled water for 1 h while in a saturated state, then cooled in the same beaker to 20 °C. After cooling, the specimens were conditioned in desiccators at 22, 42, 59, and 80 % relative humidity (RH) for three weeks at a constant temperature of 20 °C. The humidity levels were monitored using a resistance molecular membrane sensor (SHA-3151, T&D Corp., Matsumoto, Japan).

2.2 Humidity control system and dynamic viscoelasticity measurements

The humidity in the test chamber was controlled using a water vapor generator (HC9700, Netzsch Japan K.K., Kanagawa, Japan). Dry and water-saturated nitrogen gas were mixed to create an arbitrary humidity level, and the resulting moist gas was introduced into a 70 mL test chamber at a flow rate of 200 mL/min. A capacitive proximity sensor (TI-A, Toplas Engineering Co. Ltd., Tokyo, Japan) was used to measure the humidity within the chamber. To verify

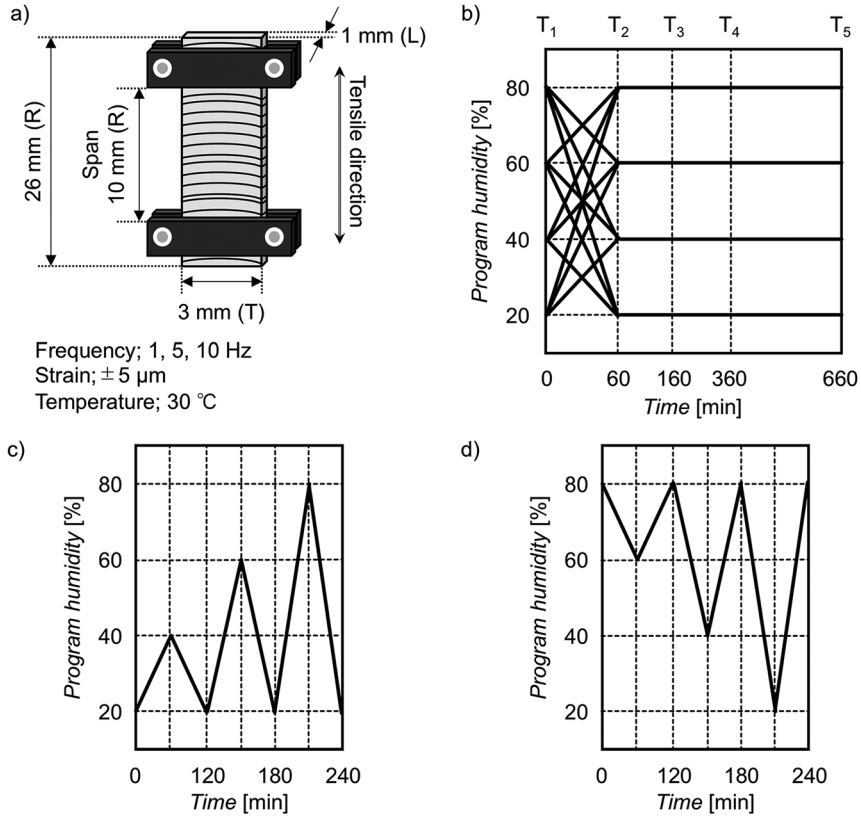

Figure 1: Description of humidity tests. (a) Schematic diagram of the sample attached to the forced-vibration dynamic mechanical analyzer. Humidity program over time for (b) dynamic viscosity, (c) adsorption, (d) and desorption experiments. *T*1: start of humidity change; *T*2: end of humidity change; *T*3, *T*4, and *T*5: 100, 300, and 600 min after *T*2, respectively, at constant humidity.

the accuracy of the humidity control, humidity changes were monitored without the specimens, with the change rate set between 0.1 and 1.0 % RH/min to ensure that the measured humidity matched the desired program settings.

Dynamic viscoelasticity measurements were performed using a forced vibration dynamic mechanical analysis system (DMA 242E Artemis, Netzsch Japan K.K., Kanagawa, Japan). Measurements were performed at sine wave frequencies of 1, 5, and 10 Hz, with a forced strain of ±5 μm, a span of 10 mm, and a constant chamber temperature of 30 °C (Figure 1a). Before measurement, the stabilization time for the specimens was determined. It was found that after 3 h, the temperature, humidity, and specimen dimensions were stabilized. Thus, a holding time of 6 h was used to ensure stability before measurement.

2.3 Humidity change programs

The humidity change program in Figure 1b was used to study the temporal variations in dynamic viscoelasticity after reaching each humidity level. The programs started with a specific RH value 20, 40, 60, and 80 %, which were changed to 20, 40, 60 %, and 80 % (excluding the initial value). For example, the initial 40 % state was decreased to 20 % and increased to 60 and 80 % RH. Figure 1c and d show additional humidity change programs designed to examine the effects of humidity change history on dynamic viscoelasticity. In all three programs, the humidity-change steps were performed over a standard 60-min transition time. The humidity changes over time in the test chamber, and the dimensional changes (ΔL) of the specimens were measured. Here, ΔL represents the percentage dimensional change relative to the initial one between the chucks at *T*1, with positive values indicating expansion and negative values indicating contraction.

Figure 2 compares the RH changes in the test chamber, as controlled by the program in Figure 1b, with the ΔL of the specimens measured in the *R* direction. These results suggest that water molecules were adsorbed or desorbed by the wood as the humidity in the chamber increased or decreased.

2.4 Moisture content of the specimens

It is hard to measure the weight change of a specimen in the chamber during dynamic viscoelasticity measurements. Therefore, to monitor the moisture content of the specimens during humidity conditioning, the specimens were quickly removed from the chamber, and their weight was measured in a chamber with a humidity change program

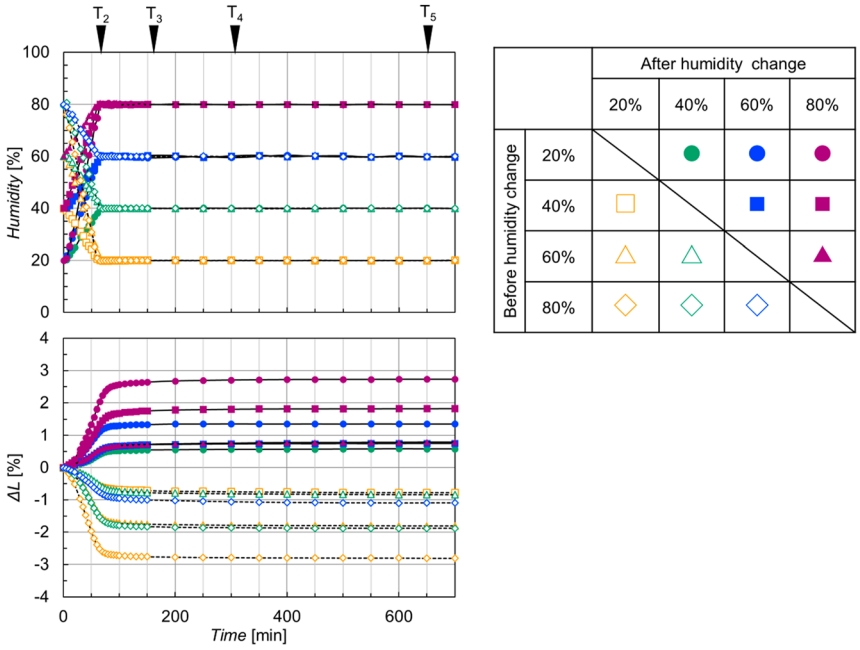

Figure 2: Changes in (a) humidity and (b) sample dimensions in the *R* direction over time during the experiments at each humidity. Filled data points & solid line: adsorption; open data points & dotted line: desorption.

similar to that used for dynamic viscoelasticity measurements. The oven-dry weight was determined after drying the specimens for 3 days at 30 °C and 0.1 MPa in a reduced-pressure dryer containing phosphorus pentoxide. This weight and those of the wet samples were used to calculate the moisture content.

The average moisture contents of the samples (n = 3) in the test chamber immediately before the humidity change (at $T1$) were 5.7 ± 0.06 % (20 %RH), 7.5 ± 0.04 % (40 %RH), 11 ± 0.10 % (60 %RH), and 15 ± 0.09 % (80 %RH). The moisture content immediately after the humidity change ($T2$) was 7.4 % (40 %RH), 10.9 % (60 %RH), and 14 % (80 %RH) during humidification (n = 1–3), and 5.8 % (20 %RH), 7.6 % (40 %RH), and 11 % (60 %RH) during dehumidification (n = 1–3). Comparing the moisture content at $T2$ and $T5$ revealed minimal fluctuations, suggesting that the specimens maintained stable moisture levels. Additionally, the weights of the specimens used for dynamic viscoelasticity and moisture content measurements at $T5$ were comparable, indicating consistent equilibrium moisture content across tests.

3 Results

3.1 Dynamic viscoelasticity of wood conditioned for three weeks

To gain insights into the changes in mechanical properties related to humidity fluctuations, particularly from the perspective of energy barriers, the mechanical properties at various humidity levels were first examined under a constant temperature of 30 °C. Measurements of the storage modulus (E'), loss modulus (E''), and loss tangent (tanδ) were taken at $T1$ (as defined in Figure 1b) for specimens conditioned at each humidity level for three weeks. These results (Figure 3), henceforth referred to as the control values, represent the equilibrium values of the specimens conditioned for the longest duration in these experiments.

The tanδ, E', and E'' values at 1 Hz presented in Figure 3 were compared with those reported by Becker and Noack (1968). The tanδ value rose when the humidity changed from 20 to 40 %RH and from 60 to 80 %RH, with minimal difference between 40 and 60 %RH. Becker and Noack's results similarly demonstrated a higher logarithmic damping ratio at a moisture content of 12 % compared to 8 % (From the moisture content measurements in this study, 12 % moisture content corresponds to 60–80 %RH in this study, and 8 % moisture content corresponds to 40–60 %RH in this study). As illustrated in Figure 3, the E' reduced as RH elevated, with the most significant reduction occurring in the 60–80 %RH range. This pattern is consistent with Becker and Noack's dynamic torsional modulus measurements and the established relationship between elastic modulus and moisture content (Kajita et al. 1961). The E'' curve shows a convex peak as a function of humidity, with the maximum value at 40 %RH. As the frequency increased, the slope of tanδ became steeper, and the E'' peak shifted to higher humidity levels.

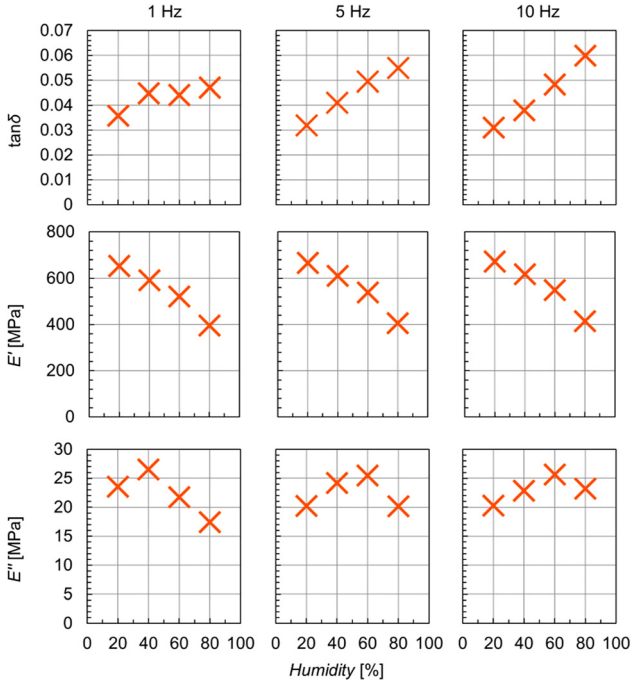

Figure 3: Humidity dependence of tanδ, E', and E'' at each tested frequency at 30 °C for wood samples moisture-conditioned over 3 weeks. These results were used as control values.

3.2 Comparison of the dynamic viscoelastic properties of wood during humidity changes and wood conditioned for three weeks (control)

Figure 3 illustrates the relationship between humidity and equilibrium conditions of tanδ, E', and E'', which were used as the standard values of the experimental system. The following discussion focuses on the behavior of tanδ, E', and E'' during the adsorption and desorption processes relative to the control values. Figures 4 and 5 compare the dynamic viscoelasticity measured during the adsorption and desorption processes, from $T1$ to $T2$ in Figure 1b, with the values for control specimens conditioned over a long period. For the adsorption process, the results are presented as relative values normalized to the value at 20 %RH, whereas for the desorption process, the results were normalized to the value at 80 %RH.

During the adsorption process (Figure 4), relative E' was higher than the control for humidity values above 60 %RH at all frequencies. However, the differences in tanδ and relative E'' between the control and the test specimens were dependent on both humidity and frequency. In the humidity range of 20–40 %RH, tanδ and relative E'' were equal to or slightly higher than the control values at all frequencies. In contrast, at humidities above 40 %RH, the relative E'' values were significantly different from the control at all frequencies. Tanδ also exhibited notable differences from the control at 1 Hz in the humidity range above 40 %RH; however, at 5 Hz and 10 Hz, the values were nearly identical to the control.

During the desorption process (Figure 5), the tanδ values were greater than the control values at all frequencies, while the relative E' values were lower than the control values at all frequencies. In contrast, relative E'' fluctuated with humidity, exhibiting values that were equal to or slightly higher than those of the control.

3.3 Rate of stabilization over time at each humidity after adsorption and desorption

In order to further analyse the results shown in Figures 4 and 5, the temporal stabilization of the molecular state of the

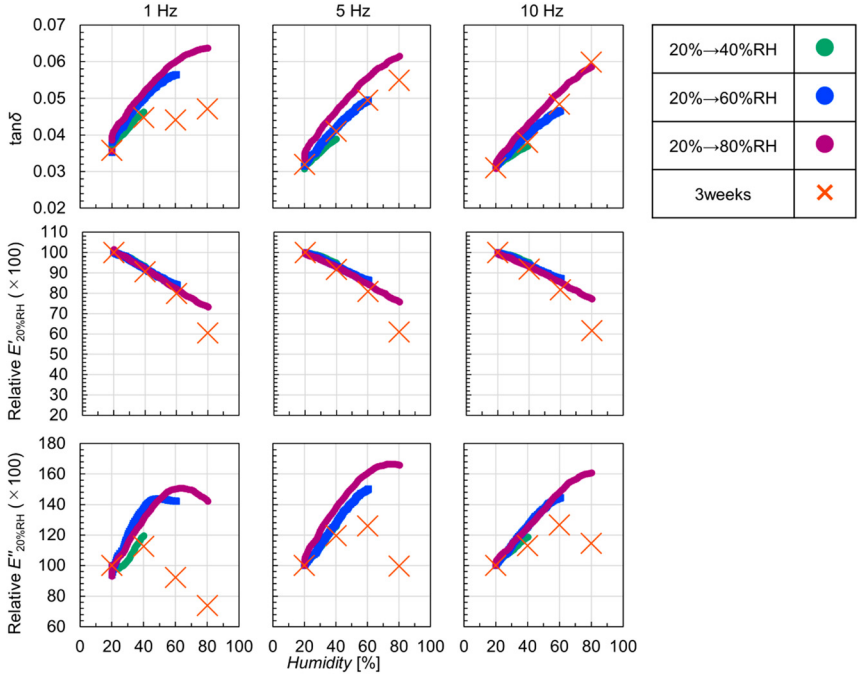

Figure 4: Comparison of tanδ, relative E', and relative E'' values of wood measured under adsorption conditions with the control curves. Note: Relative values are based on values at 20 % RH.

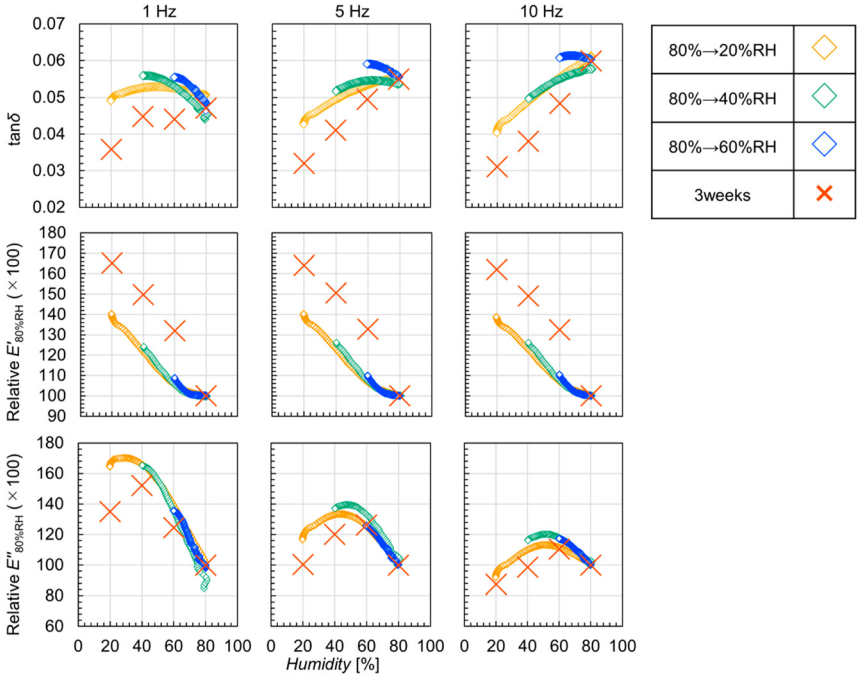

Figure 5: Comparison of tanδ, relative E', and relative E'' values of wood measured under desorption conditions with the control curves. Note: Relative values are based on values at 80 % RH.

wood must be considered, starting from immediately after adsorption and desorption in the horny layer. In previous research, tanδ/tanδ was used to show the extent to which an arbitrary unstable state is distant from a stable state (Miyoshi et al. 2020). Figure 6 compares the extent to which tanδ at different times ($T2$, $T3$, $T4$) approaches tanδ at $T5$, as calculated by the following formula:

$$\tan\delta_i / \tan\delta_{T5} = (\tan\delta \text{ at time } i / \tan\delta \text{ at time } T5) \times 100 \ (i = T2, T3, T4)$$

When this value is close to 100, the difference between the numerator and denominator is small, indicating a high degree of similarity to tanδ at time $T5$. In addition, $\tan\delta_i/\tan\delta_{T5}$ represents the ratio of tanδ at each humidity to $\tan\delta_{T5}$ (the loss tangent when the wood itself is relatively stable), which is close to the net molecular momentum at each time point. Therefore, the decrease in $\tan\delta_i/\tan\delta_{T5}$ can reflect the behavior of the unstable microstructure, which stabilizes over time following adsorption and desorption due to the molecular mobility of the wood at that humidity and time.

Figure 6 shows the decline in $\tan\delta_i/\tan\delta_{T5}$ over time following adsorption. At 1 Hz, the ratio decreased progressively from $T2$ to $T4$ for all humidity levels (40–80 %RH). The most significant decrease occurred in the 20 %RH → 80 %RH transition, followed by the 20 %RH → 60 %RH and 20 %RH → 40 %RH transitions. When comparing the decrease in $\tan\delta_i/\tan\delta_{T5}$ at 20 %RH → 80 %RH across different frequencies, the greatest decline was observed at 1 Hz, while at 5 and 10 Hz, the ratio remained only slightly below 100 %.

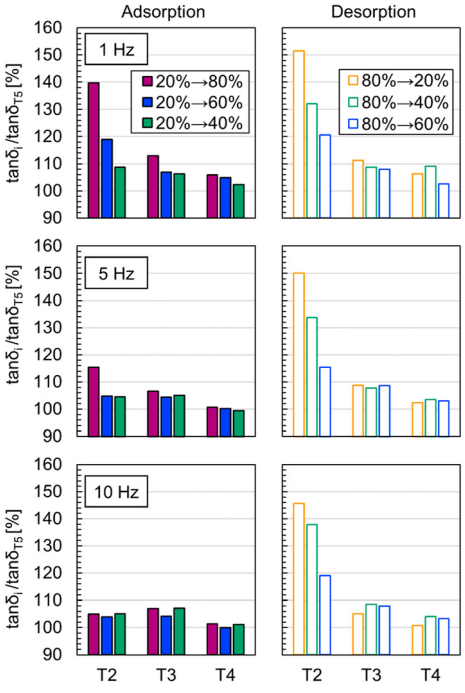

Figure 6: Degree of stabilization at various humidity levels after humidity change. Note: $\tan\delta_i/\tan\delta_{T5}$ (i = $T2$, $T3$, $T4$) percentages are based on $T5$ (600 min after $T2$), indicating how close the values are to that measured at the stable $T5$ state after changes in humidity.

Similarly, for the 20 %RH → 60 %RH and 20 %RH → 40 %RH transitions, a decreasing trend was observed at 1 Hz, but the values at 5 and 10 Hz remained slightly higher than 100 %. In contrast, the decrease in $\tan\delta_i/\tan\delta_{T5}$ over time following

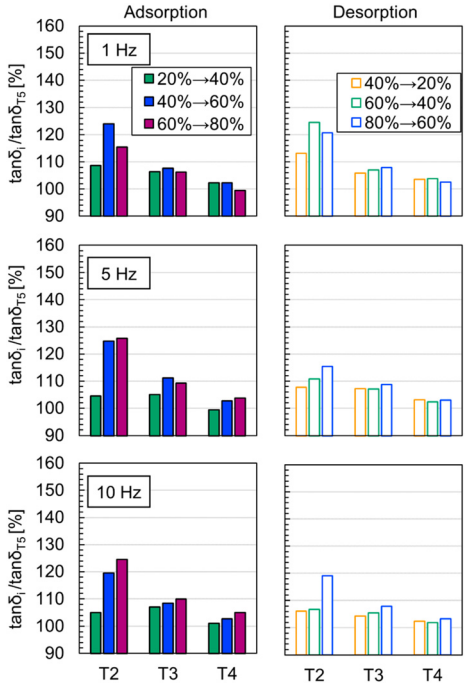

Figure 7: Change of $\tan\delta_i/\tan\delta_{T5}$ (i = $T2$, $T3$, $T4$) over time after adsorption/desorption in each humidity range.

desorption exhibited a different trend to that observed for the adsorption process. In all cases, a decline was observed from $T2$ to $T4$, with a greater decrease as the range of humidity change increased.

Furthermore, the changes in $\tan\delta_i/\tan\delta_{T5}$ for different RH values but a fixed change in humidity of 20 %RH were examined (Figure 7). The largest decreases in $\tan\delta_i/\tan\delta_{T5}$ from $T2$ to $T4$ were observed at 1 Hz for the humidity changes of 40 % ↔ 60 %RH, 60 % ↔ 80 %RH, and 20 % ↔ 40 %RH, respectively. At 5 and 10 Hz, the decreasing trend followed the order of 60 % ↔ 80 %RH, 40 % ↔ 60 %RH, and 20 % ↔ 40 %RH, respectively. Additionally, comparisons were made between transitions with the same humidity change range and final humidity levels, such as 20 % → 40 %RH and 60 % → 40 %RH, as well as 40 % → 60 %RH and 80 % → 60 %RH. At 1 Hz, $\tan\delta_i/\tan\delta_{T5}$ followed the order $T2 \rightarrow T3 \rightarrow T4$.

3.4 Transition in mechanical properties around the medium humidity (30–60 %RH)

Section 3.1 described the observed peak in E'' around the medium humidity. This peak may represent a turning point that significantly alters the mechanical properties of wood, suggesting that molecular mobility may differ between the low and high humidity ranges, with the medium humidity as the threshold value. To further clarify the behavior of the wood as it transitions through this point during the adsorption and desorption processes, experiments were conducted in which humidity was gradually increased and decreased (Figure 1c) or decreased and increased (Figure 1d). This humidity change program passes through each of the humidity levels of 20, 40, 60, and 80 %RH in a given molecular state and assumes that the molecular state at that time is recorded. For example, in the case of a humidity change program of 20 %RH → 40 % RH → 20 %RH → 60 %RH, molecular motion is activated by water adsorption during the transition from 20 to 40 %RH, and the molecular state during the relaxation process at 40 %RH is "frozen" during desorption from 40 to 20 %RH. It can be predicted that the molecular state at 20 %RH will be reached while maintaining the accumulated unstable state during the adsorption/desorption process of 20 %RH to 40 %RH to 20 %RH and that the molecular motion will be reactivated during the transition from 20 to 60 %RH.

To demonstrate the tracking performance of this humidity change program, Figure 8 shows the changes over time in the RH of the chamber and the ΔL of the test piece. As the specimen expands and contracts in response to the ambient humidity, it is judged to be tracking with little effect from diffusion.

Figures 9 and 10 compare the dynamic viscoelasticity of wood during stepwise adsorption and desorption with the control values. Relative values are shown based on 20 %RH for the adsorption process (Figure 9) and on 80 %RH for the desorption process (Figure 10).

During the adsorption process (Figure 9), $\tan\delta$, relative E', and relative E'' did not significantly deviate from the control values in the 20 → 40 → 20 %RH cycle at all frequencies. Additionally, relative E' only showed minor deviations from the control values during adsorption in the humidity range above 60 %RH at all frequencies. However, the humidity at which relative E'' deviated from the control varied was frequency dependent. At 1 Hz, relative E'' deviated from the control when the RH exceeded 40 % during the 20 % → 60 %RH transition, after which the values oscillated above the control. At 5 and 10 Hz, relative E'' moved away from the control when the RH exceeded 60 % during the 20 % → 80 %RH transition and continued fluctuating above the control value.

During the desorption process (Figure 10), the relative E' at all frequencies deviated from the control immediately after desorption and fluctuated between smaller values. Relative E' also showed larger values during adsorption than desorption, eventually approaching the control. However, the behavior of relative E'' depended on the frequency and humidity. At 1 Hz, relative E'' did not deviate during the 80 % → 60 %RH transition but showed deviations during re-adsorption from 60 to 80 %RH. During desorption from 80 to 40 %RH, the behavior of relative E'' between 80 and 60 %RH showed a distinct

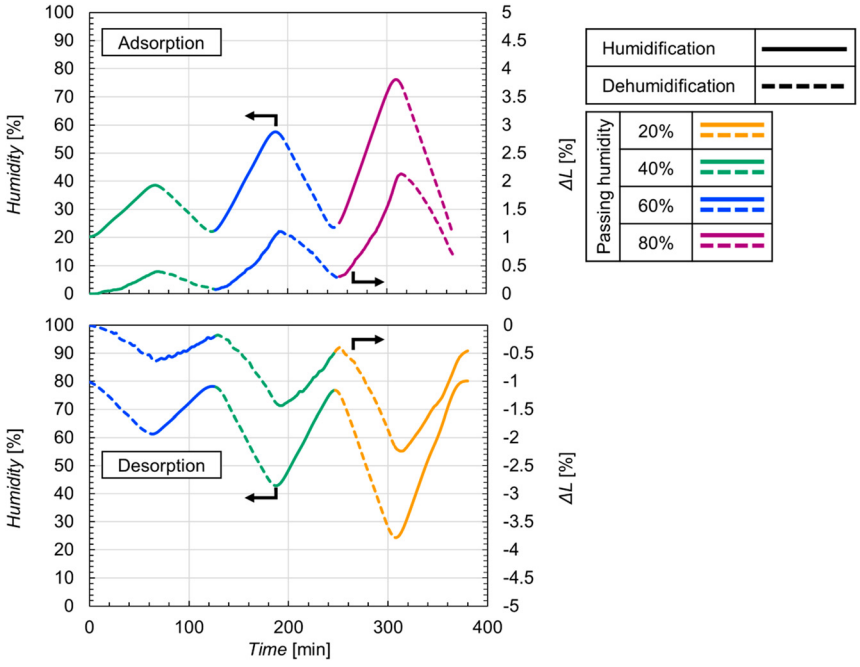

Figure 8: Time dependence of humidity and dimensional change (Δ*L*) during the humidity history experiments under adsorption/desorption conditions. Lines and colors follow Figure 2. "Passing humidity" means a process where the humidity increases up to a specific level and then returns to the original value.

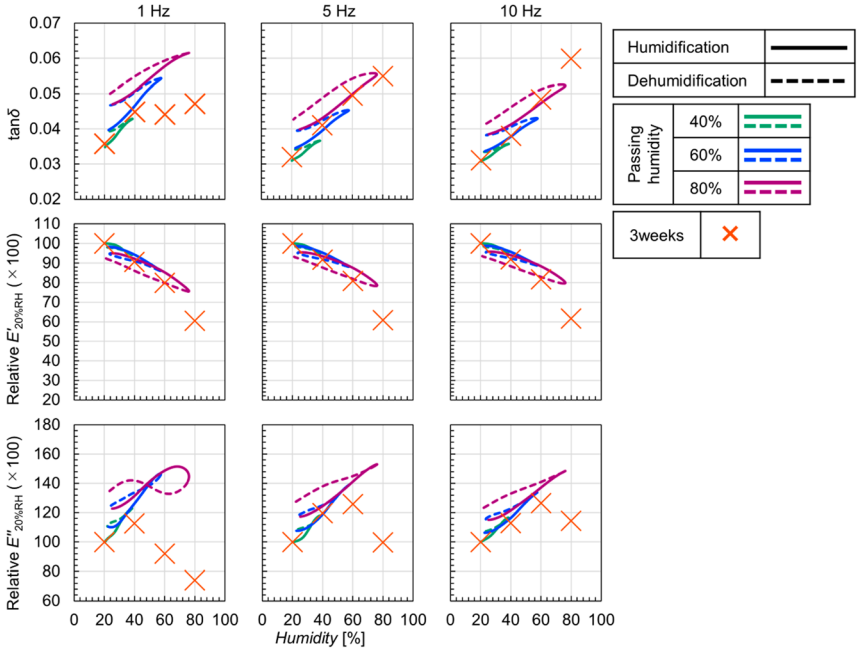

Figure 9: Influence of adsorption humidity range on dynamic viscoelasticity of destabilized wood. Lines and colors follow Figure 2; cross follows Figure 3.

difference compared to the re-adsorption cycle (60–80 % RH), where the values were consistently larger than the control and did not overlap with any points obtained during the humidity change history. At 5 and 10 Hz, relative E'' remained close to the control values, but during desorption from 80 %RH to 40 %RH, overlapping behavior with the 80 % → 60 %RH transition was observed, as seen at 1 Hz.

4 Discussion

Based on the thermal softening properties of wood in a swollen state, the relaxation of amorphous polysaccharides (hemicellulose) and relaxation due to the micro-Brownian motion of lignin, have been observed at approximately −50 and 80 °C, respectively (Furuta et al. 1997, 2001; Salmén 1984). The relaxation observed around 80 °C in the water-swollen

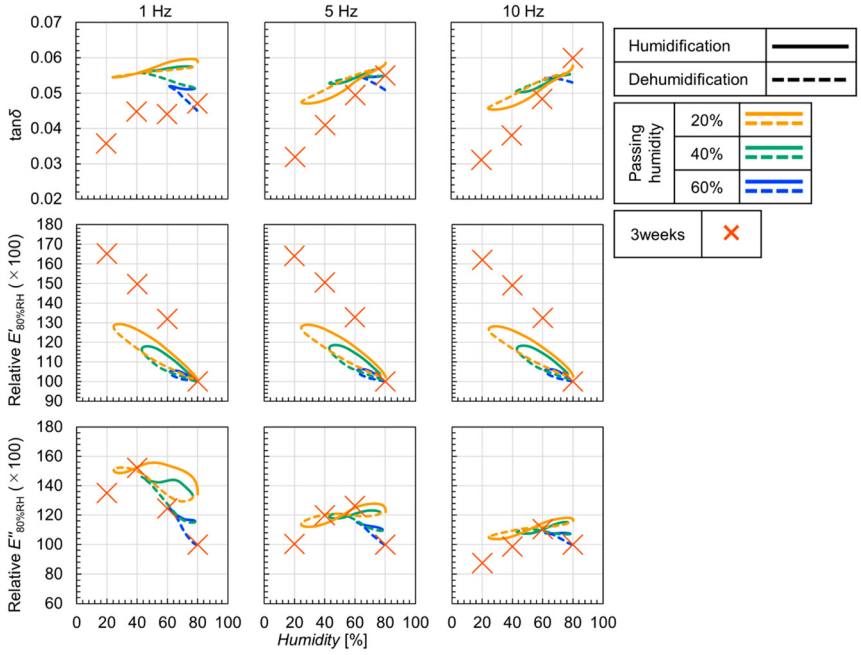

Figure 10: Influence of desorption humidity range on dynamic viscoelasticity of destabilized wood. Lines and colors follow Figure 2; cross follows Figure 3.

state is considered to correspond to the glass transition temperature of lignin (Furuta et al. 2008, 2010). This glass transition temperature marks the boundary between the low-temperature glassy state and the high-temperature rubbery state. As the moisture content decreases, the glass transition temperature shifts to higher temperatures, and below 12 % moisture content, it no longer appears below 100 °C, i.e., in the range of liquid water (Becker and Noack 1968). Thus, since the experiments in this study were performed at ~30 °C, lignin is expected to be in a glassy state. It is further hypothesized that as the moisture content increases or decreases, lignin transitions within the glassy state from a condition far from the rubbery state to one that is closer to it. Therefore, the results are discussed considering the molecular state of lignin at a constant 30 °C over time.

During the adsorption process, the interaction between molecular chains in the amorphous region of the wood weakens due to the adsorption of water molecules, so the molecular motion of the wood becomes more active, but the opposite phenomenon occurs during the desorption process. In this study, it is also expected that this phenomenon will occur during the humidity change process ($T1 \rightarrow T2$). At all frequencies, relative E' values during adsorption were consistent with the control values between 20 and 60 %RH, while during desorption, they deviated immediately after humidity reduction (Figures 4 and 5). This observation also explains the behavior of tanδ at 1 Hz during adsorption and at 1–10 Hz during desorption. However, it does not fully explain the behavior of relative E'' in response to humidity changes or the behavior of tanδ at 5 and 10 Hz during adsorption. The differences at 5 and 10 Hz during adsorption are thought to be due to variations in molecular mobility at different molecular scales and may be related to differences in the strain experienced by molecular chains due to humidity changes.

To further compare the strain over time after adsorption and desorption at each RH, tanδ values measured immediately after the humidity change ($T2$) or 600 min after ($T5$) were examined in detail as they approached a stable state. The molecular state immediately after adsorption ($T2$) represents the relaxation process following activation, while the molecular state immediately after desorption represents relaxation following deactivation. The molecular state after adsorption relaxes more easily than that after desorption, as molecular motion is activated to a higher degree. The results measured at higher frequencies are thought to reflect processes at smaller molecular scales (Nielsen 1976). For the measurements at 5 and 10 Hz, $\tan\delta_i/\tan\delta_{T5}$ was already close to 100 % at $T2$, indicating that relaxation had already occurred by that time (Figure 6). This is supported by the results for 5 and 10 Hz in Figure 4. In contrast, no significant difference in the changes in $\tan\delta_i/\tan\delta_{T5}$ during desorption was observed, suggesting that molecular deactivation proceeded uniformly across different molecular scales. The largest changes in $\tan\delta_i/\tan\delta_{T5}$ during desorption were observed in the order of 80 → 20 %RH, 80 → 40 %RH, and 80 → 60 %RH. This indicates that the magnitude of the humidity change plays a role, although further investigation is needed to draw definitive conclusions.

In Figure 7, the decrease in $\tan\delta_i/\tan\delta_{T5}$ from $T2$ to $T4$ was most pronounced at 1 Hz for humidity changes between

40 % ↔ 60 %RH, 60 % ↔ 80 %RH, and 20 % ↔ 40 %RH. At 5 and 10 Hz, the decrease in $\tan\delta_i/\tan\delta_{T5}$ followed the order of 60 % ↔ 80 %RH, 40 % ↔ 60 %RH, and 20 % ↔ 40 %RH. From the perspective of molecular mobility, the time required for strain resolution should be shorter for high RH ranges, where moisture adsorption is greater. Furthermore, wood after adsorption should relax faster than wood immediately after desorption. Thus, the decrease in $\tan\delta_i/\tan\delta_{T5}$ measured at 5 and 10 Hz for the humidity-change process suggests a faster relaxation rate at higher RH ranges. However, the large decrease in $\tan\delta_i/\tan\delta_{T5}$ at 1 Hz from $T2$ to $T4$ at 60 % ↔ 80 %RH cannot be fully explained by the molecular mobility of lignin alone. It is therefore hypothesized that an additional energy barrier, beyond that associated with lignin, exists in the humidity range around the medium humidity.

Examining the relative E'' in Figure 9 shows that once the E'' peak of the control is exceeded in the adsorption direction, the values remain higher than the control. In Figure 10, although the E'' peak of the control was not exceeded, the values still increased during the first re-adsorption process after desorption. In addition, E' did not decrease rapidly at around 60 %RH, and in the adsorption direction, it repeated the same change path, while in the desorption direction, the change path was different. Based on the above assumptions, it is believed that the fine structure of wood transitions from a glassy to a rubbery state through repeated adsorption and desorption cycles when the energy barrier is exceeded in the adsorption direction and reverts to the glassy state when the barrier is exceeded during desorption. However, the original glassy state cannot be fully restored because molecular motion becomes highly activated in the rubbery state. Based on these results, an energy barrier is believed to exist around the medium humidity.

Finally, the other factors contributing to the energy barrier around the medium humidity are considered in light of previous research (Cousins 1976, 1978; Kollmann 1962; Kulasinski et al. 2014; Obataya et al. 1996; Olsson and Salmén 2003; Simpson 1971, 1980; Yokoyama et al. 1999, 2000a,b). Numerous reports have described transitions in physical and mechanical properties within this humidity range, suggesting that this phenomenon is not unique to the current experimental system. For example, it has been reported that isolated hemicellulose undergoes thermal softening at around 60 %RH at room temperature (Goring 1963; Takamura 1968). Additionally, mechanical relaxation in the low-temperature region is associated with the state of water in the wood, and it has been suggested that the mechanical relaxation of wood in the swollen state shifts toward room temperature as the material dries (Furuta et al. 2001; Obataya et al. 1996; Yokoyama et al. 2000a,b). Moreover, it has been reported that the dynamic viscoelasticity of isolated hemicellulose depends on the frequency during the process of humidity change (Olsson and Salmén 2003). Thus, a change in the molecular state of hemicellulose is likely to occur. However, the thermal softening of hemicellulose is difficult to detect due to restricted molecular motion caused by its binding to the cellulose surface, despite the chain-like nature of xylan between cellulose and lignin (Salmén 2022). Furthermore, the activation energy for the thermal softening of amorphous polysaccharides is low for the micro-Brownian motion of hemicellulose at around −50 °C (Furuta et al. 2001). Therefore, the changes in the physical and mechanical properties of wood in the moderate humidity range during humidity cycling cannot be conclusively attributed to the mechanical relaxation of hemicellulose alone.

To comprehensively interpret the results of this and previous studies, it is reasonable to conclude that changes in molecular mobility due to the glass transition of lignin, along with changes in the state of amorphous polymers within the wood cell wall caused by hemicellulose softening, are involved. However, further investigation is necessary to fully clarify the effect of hemicellulose softening on the energy barrier around the medium humidity.

5 Conclusions

To help clarify the mechanism of changes in the mechanical properties of wood caused by water adsorption and desorption, the viscoelastic properties of the wood were considered from the perspective of polymer rheology and an energy barrier. This study is based on the fact that, at a constant temperature, higher moisture contents reduce the glass transition temperature derived from lignin. The difference between a constant temperature of 30 °C and the glass transition temperature changes during the adsorption and desorption processes. During the adsorption process, it approaches the glass transition temperature (transitioning from a glassy state that is far from a rubber state to a glassy state that is close to a rubber state), and the reverse occurs during the desorption process. A detailed analysis of the mechanical properties of the wood under adsorption and desorption processes explained the previously unexplained changes in molecular mobility within the wood cell wall without contradiction. However, E'' during adsorption and desorption at the medium humidity, the time variation of $\tan\delta$ after adsorption above the medium humidity, and the increase in molecular motion cannot be explained by the aforementioned assumptions. These behaviors could be consistently explained by assuming that not only a slight energy barrier due to lignin but also the softening of

hemicellulose around the medium humidity was responsible for the change in the state of the amorphous polymer in the wood cell wall. Therefore, the findings confirmed that an energy barrier exists around the medium humidity, which affects the dynamic viscoelastic behavior during water adsorption and desorption, but further verification is needed to clarify the hemicellulose softening phenomenon and accompanying state changes in the amorphous regions within the cell walls.

Research ethics: Not applicable.
Informed consent: Not applicable.
Author contributions: KU conducted the experiments and wrote the manuscript. YM supervised KU. HH, KK, and KY participated in the discussion of the results. YF supervised the work. All authors have accepted responsibility for the entire content of this manuscript and approved its submission.
Use of Large Language Models, AI and Machine Learning Tools: None declared.
Conflict of interest: The authors state no conflict of interest.
Research funding: No specific funding was obtained for this presented work.
Data availability: The raw data will be provided upon reasonable request from the corresponding author.

References

Armstrong, L.D. and Christensen, G.N. (1961). Influence of moisture changes on deformation of wood under stress. *Nature* 191: 869–870.

Becker, H. and Noack, D. (1968). Studies on dynamic torsional viscoelasticity of wood. *Wood Sci. Technol.* 2: 213–230.

Brémaud, I. and Gril, J. (2021a). Moisture content dependence of anisotropic vibrational properties of wood at quasi equilibrium: analytical review and multi-trajectories experiments. *Holzforschung* 75: 313–327.

Brémaud, I. and Gril, J. (2021b). Transient destabilisation in anisotropic vibrational properties of wood when changing humidity. *Holzforschung* 75: 328–344.

Cousins, W.J. (1976). Elastic modulus of lignin as related to moisture content. *Wood Sci. Technol.* 10: 9–17.

Cousins, W.J. (1978). Young's modulus of hemicellulose as related to moisture content. *Wood Sci. Technol.* 12: 161–167.

Engelund, E.T., Thygesen, L.G., Svensson, S., and Hill, C.A.S. (2013). A critical discussion of the physics of wood–water interactions. *Wood Sci. Technol.* 47: 141–161.

Furuta, Y., Yano, H., and Kajita, H. (1995). Thermal-softening properties of water-swollen wood I. The effect of drying history. *Mokuzai Gakkaishi* 41: 718–721.

Furuta, Y., Norimoto, M., and Yano, H. (1997). Thermal-softening properties of water-swollen wood V. The effect of drying and heating history. *Mokuzai Gakkaishi* 44: 82–88.

Furuta, Y., Obata, Y., and Kanayama, K. (2001). Thermal-softening properties of water-swollen wood: the relaxation process due to water soluble polysaccharides. *J. Mater. Sci.* 36: 887–890.

Furuta, Y., Nakajima, M., Nakatani, T., Kojiro, K., and Ishimaru, Y. (2008b). Effects of the lignin on the thermal-softening properties of the water-swollen wood. *J. Soc. Mater. Sci.* 57: 344–349.

Furuta, Y., Nakajima, M., Nakanii, E., and Ohkoshi, M. (2010). The effects of lignin and hemicellulose on thermal-softening properties of water-swollen wood. *Mokuzai Gakkaishi* 56: 132–138.

Goring, D.A.I. (1963). Thermal softening of lignin, hemicellulose and cellulose. *Pulp Paper Mag. Canada* 64: T517–T527.

Grossman, P.U.A. (1976). Requirements for a model that exhibits mechano-sorptive behaviour. *Wood Sci. Technol.* 10: 163–168.

Horiyama, H., Kojiro, K., Okahisa, Y., Imai, T., Itoh, T., and Furuta, Y. (2022). Combined analysis of microstructures within an annual ring of Douglas fir (*Pseudotsuga menziesii*) by dynamic mechanical analysis and small angle X-ray scattering. *J. Wood Sci.* 68: 52.

Hunt, D.G. and Gril, J. (1996). Evidence of a physical ageing phenomenon in wood. *J. Mater. Sci. Lett.* 15: 80–82.

Hunt, D.G. and Shelton, C.F. (1987). Progress in the analysis of creep in wood during concurrent moisture changes. *J. Mater. Sci.* 22: 313–320.

Iida, I., Murase, K., and Ishimaru, Y. (2002). Stress relaxation of wood during the elevating and lowering processes of temperature and the set after relaxation. *J. Wood Sci.* 48: 8–13.

Ishimaru, Y., Arai, K., Mizutani, M., Oshima, K., and Iida, I. (2001a). Physical and mechanical properties of wood after moisture conditioning. *J. Wood Sci.* 47: 185–191.

Ishimaru, Y., Narimoto, S., and Iida, I. (2001b). Mechanical properties of wood swollen in organic liquids with two or more functional groups for hydrogen bonding in a molecule. *J. Wood Sci.* 47: 171–177.

Ishimaru, Y., Oshima, K., and Iida, I. (2001c). Changes in the mechanical properties of wood during a period of moisture conditioning. *J. Wood Sci.* 47: 254–261.

Kajita, S., Yamada, T., and Suzuki, M. (1961). Studies on rheological properties of wood 1. Effect of moisture content on the dynamic-Young's modulus of wood. *Mokuzai Gakkaishi* 7: 29–33.

Kojiro, K., Furuta, Y., and Ishimaru, Y. (2008a). Influence of heating and drying history on micropores in dry wood. *J. Wood Sci.* 54: 202–207.

Kojiro, K., Furuta, Y., and Ishimaru, Y. (2008b). Influence of heating history on dynamic viscoelastic properties and dimensions of dry wood. *J. Wood Sci.* 54: 196–201.

Kojiro, K., Furuta, Y., and Ishimaru, Y. (2008c). Influence of histories on dynamic viscoelastic properties and dimensions of water-swollen wood. *J. Wood Sci.* 54: 95–99.

Kollmann, F. (1962). Eine Gleichung der Sorptionsisotherme. *Naturwissenschaften* 49: 206–207.

Kulasinski, K., Keten, S., Churakov, S.V., Guyer, R., Carmeliet, J., and Derome, D. (2014). Molecular mechanism of moisture-induced transition in amorphous cellulose. *ACS Macro Lett.* 3: 1037–1040.

Leicester, R.H. (1971). A rheological model for mechano-sorptive deflections of beams. *Wood Sci. Technol.* 5: 211–220.

Miyoshi, Y., Sakae, A., Arimura, N., Kojiro, K., and Furuta, Y. (2018). Temperature dependences of the dynamic viscoelastic properties of wood and acetylated wood swollen by water or organic liquids. *J. Wood Sci.* 64: 157–163.

Miyoshi, Y., Sakae, A., Arimura, N., Kojiro, K., and Furuta, Y. (2020). Dynamic viscoelastic properties of wood and acetylated wood in nonequilibrium states swollen by water or organic liquids. *J. Wood Sci.* 66: 6.

Miyoshi, Y., Abe, H., Horiyama, H., Kojiro, K., and Furuta, Y. (2024). Influence of habitat, density, lignin structure, and extraction treatment on thermal-softening properties of water-swollen wood: a study of 87 wood specimens. *Holzforschung* 78: 109–120.

Mukudai, J. and Yata, S. (1988). Verification of Mukudai's mechano-sorptive model. *Wood Sci. Technol.* 22: 43–58.

Nakano, T. (1996). Viscosity and entropy change in creep during water desorption for wood. *Wood Sci. Technol.* 30: 117–125.

Nielsen, L.E. (1976). *Mechanical properties of polymers and composites*. Kagaku Doujin, Kyoto.

Obataya, E., Yokoyama, M., and Norimoto, M. (1996). Mechanical and dielectric relaxations of wood in a low temperature range I. Relaxation due to methylol groups and adsorbed water. *Mokuzai Gakkaishi* 42: 243–249.

Olsson, A.M. and Salmén, L. (2003) The softening behavior of hemicelluloses related moisture. In: Gatenholm, P., and Tenkanen, M. (Eds.). *Hemicelluloses: science and technology*. ACS, Washington, D.C., pp. 184–197.

Olsson, A.M., Salmén, L., Eder, M., and Burgert, I. (2007). Mechano-sorptive creep in wood fibres. *Wood Sci. Technol.* 41: 59–67.

Salmén, L. (1984). Viscoelastic properties of in situ lignin under water-saturated conditions. *J. Mater. Sci.* 19: 3090–3096.

Salmén, L. (2022). On the organization of hemicelluloses in the wood cell wall. *Cellulose* 29: 1349–1355.

Salmén, L., Stevanic, J.S., and Olsson, A.M. (2016). Contribution of lignin to the strength properties in wood fibres studied by dynamic FTIR spectroscopy and dynamic mechanical analysis (DMA). *Holzforschung* 70: 1155–1163.

Simpson, W.T. (1971). Equilibrium moisture content prediction for wood. *For. Prod. J.* 21: 48–49.

Simpson, W. (1980). Sorption theories applied to wood. *Wood Fiber Sci.* 3: 183–195.

Skaar, C. (1988). *Wood-water relations*. Springer-Verlag, Berlin.

Takahashi, C., Ishimaru, Y., Iida, I., and Furuta, Y. (2004). The creep of wood destabilized by change in moisture content. Part 1: The creep behaviors of wood during and immediately after drying. *Holzforschung* 58: 261–267.

Takahashi, C., Ishimaru, Y., Iida, I., and Furuta, Y. (2005). The creep of wood destabilized by change in moisture content. Part 2: The creep behaviors of wood during and immediately after adsorption. *Holzforschung* 59: 46–53.

Takahashi, C., Ishimaru, Y., Iida, I., and Furuta, Y. (2006). The creep of wood destabilized by change in moisture content. Part 3: The influence of changing moisture history on creep behavior. *Holzforschung* 60: 299–303.

Takamura, N. (1968). Studies on hot pressing and drying process in the production of fiberboard 3. Softening of fibre components in hot pressing of fibre mat. *Mokuzai Gakkaishi* 14: 75–79.

Takemura, T. (1968). Plastic properties of wood in relation to the non-equilibrium states of moisture content (re-continued). *Mokuzai Gakkaishi* 14: 406–410.

Thybring, E.E., Fredriksson, M., Zelinka, S.L., and Glass, S.V. (2022). Water in wood: a review of current understanding and knowledge gaps. *Forests* 13: 2051.

Tokumoto, M. (2001). Bending creep and set of small wood beams during adsorption and desorption cycles. *Mokuzai Gakkaishi* 47: 189–197.

Yokoyama, M., Obataya, E., and Norimoto, M. (1999). Mechanical and dielectric relaxations of wood in a low temperature range II. Relaxation due to adsorbed water. *Mokuzai Gakkaishi* 45: 95–102.

Yokoyama, M., Kanayama, K., Furuta, Y., and Norimoto, M. (2000a). Mechanical and dielectric relaxations of wood in a low temperature range III. Application of sech law to dielectric properties due to adsorbed water. *Mokuzai Gakkaishi* 46: 173–180.

Yokoyama, M., Ohmae, K., Kanayama, K., Furuta, Y., and Norimoto, M. (2000b). Mechanical and dielectric relaxations of wood in a low temperature range IV. Dielectric properties of adsorbed water at high moisture contents. *Mokuzai Gakkaihi* 46: 523–530.